Published in the PSCC 2018 proceedings, ©IEEE

# System Properties of Packetized Energy Management for Aggregated Diverse Resources

Luis A. Duffaut Espinosa, Mads Almassalkhi, Paul Hines, Jeff Frolik
Department of Electrical and Biomedical Engineering
University of Vermont, Burlington, VT 05405 USA
{lduffaut, malmassa, phines, jfrolik}@uvm.edu

***Abstract*—This paper presents the systematic analysis of a population of diverse distributed energy resources (DERs) coordinated using a bottom-up approach known as packetized energy management (PEM). Particularly, for the aggregation of DERs modeled as a bilinear system, a simple discrete-time control law is provided that maximizes the number of accepted requests while tracking a regulation signal provided by a regional transmission operator. Moreover, the mechanics of energy packet completion rates under persistent inputs and the definition of a nominal quality of service (QoS) controller for PEM are provided. Finally, the observability of the PEM system is addressed including an implementation of the extended Kalman filter (EKF) for state estimation of the dynamic state of a diverse DER population.**

***Index Terms*—Flexibility, distributed energy resources, packetized energy management, observability, modeling.**

## I. Introduction

At high levels of renewable generation, today's operating paradigm for reliably managing the variability of wind and solar generation requires having more responsive energy resources. One way to provide such resources is to consider an active role for flexible and controllable net-load energy resources at the residential level, e.g., thermostatically-controlled loads (TCLs), energy storage systems (ESSs), and plug-in electric vehicles (PEVs). While the core concepts underlying modern demand-side management (DSM) have existed for decades, the technology for aggregating and choreographing distributed energy resources (DERs) is nascent [1], [2].

**Literature Review:** More recently, the authors in [3] illustrated how controllable loads could be used in transmission and distribution system operations to manage the variability from renewables. The work in [4] expanded on these principles by injecting randomization into the control of a state bin transition model for a (homogeneous) population of TCLs. An $N$-dimensional control input is computed and broadcast in top-down fashion to all devices. The control input defines the ON/OFF switching probabilities for each of $N$ temperature bins and devices then map their local temperature to a binned value and switch ON/OFF with given probability. While this framework depends on solving a challenging bilinear state-estimation problem and may not always be observable [5], it has been analyzed and extended to include interesting use cases [6]–[8]. Related works with state bin transition models of TCLs have also focused on higher order models [9], compressor constraints [10], and analyzing the modeling uncertainty resulting from heterogeneous populations [11]. Work by [5] offers an interesting alternative approach of employing mean-field control to develop a SISO model of a (homogeneous) fleet of pool-pumps [12] or batteries [13]. The mean-field approach leverages a local randomized control policy whereby the central coordinator computes and broadcasts (in top-down fashion) a scalar control input that perturbs each device's local ON and OFF state transition rates to regulate the fleet's aggregate power output. The authors have extended this work to consider estimation of quality-of-service (QoS) and opt-out control modes [14]. Nonetheless, the mean field approach depends crucially on a baseline response that may be challenging to validate. A second order linear model of TLCs is developed in [15], where direct load control (DLC) of air conditioners (A/Cs) is investigated for variable ambient conditions and offers an intriguing path for system identification of heterogeneous systems.

PEM leverages packet-based strategies from random access communication channels, which have previously been applied to the distributed management of wireless sensor networks (i.e., a multi-channel ALOHA protocol). Under PEM, energy is delivered to a load via multiple fixed-duration/fixed-power "energy packets," similar to how digital communication networks break files into data packets. In contrast to those prior works, PEM does not broadcast a control signal (in top-down fashion). Instead, PEM is designed to have each load request an energy packet from the coordinator stochastically based on the loads local dynamic state (in a bottom-up fashion). The central coordinator then responds in real-time to each packet request based on grid or market conditions. Related work on energy packets is given by [16], where a distributed (binary information) packet control algorithm is proposed that requires just binary information from each load at each time instant. The main drawbacks of the binary control protocol are the assumption of complete knowledge of the exact number of participating packetized loads at any given time, the authorization of packet requests from the queue is synchronized, and the queue stores packet requests if the packets cannot be allocated, which creates delays in service. Other discrete "packet" scheduling algorithms include the regulation of discrete energy demands in [17] and an IoT-inpired approach to regulate discrete step-changes in temperature set-points for a population of A/Cs [18].

This paper presents systematic analysis for a model of the aggregate system response (i.e., a bilinear discrete-time Markov chain) of a population of diverse classes of DERs, including TCLs and ESSs.

This work was supported by the U.S. Department of Energy's Advanced Research Projects Agency - Energy (ARPA-E) award DE-AR0000694. M. Almassalkhi, P. Hines, and J. Frolik are co-founders of startup Packetized Energy, which seeks to bring to market a commercially viable version of Packetized Energy Management. This work was also partially supported by NSF grant IIP-1722008.

**Contributions:**

- A simple mean-field-inspired control law is implemented for real-time tracking of reference power signals. This control law modulates packet acceptance ratios which allows PEM to correct tracking errors with only a three inputs: aggregate power, number of charging requests, and number of discharging requests. Here, it is shown that PEM can minimize tracking error while maximizing the acceptance of requested charging and discharging energy packets.
- Calculating flexibility levels depends on the mechanism for expiring packets, which is handled by two deterministic timers within the PEM scheme. A theoretical upper bound on expiring packet ratios is derived and it is shown that the proportion of packets that are expiring does not vary significantly during tracking if the system is not stressed (i.e., DERs do not opt-out of PEM *en masse*).
- The nominal response of the PEM system is explicitly characterized in terms of a stationary distribution in a manner that QoS constraints are satisfied for the average residential DER owner.
- Finally, observability of the bilinear discrete-time model that underpins PEM is investigated. An Extended Kalman Filter is deployed to estimate the dynamic distribution of a diverse DER population.

The paper is organized as follows. Section II provides a succinct summary about PEM and the aggregated model. In Section III, a reference-tracking controller that maximizes the number of accepted requests is presented. Properties of the PEM system related to mechanics of packet completion rates and nominal quality of service (QoS) control is presented in Section IV. Section V studies observability and provids an EKF implementation for the PEM system. The final section concludes the paper.

## II. Packetized Energy Management Preliminaries

At the local level, DERs manage packet requests similarly to how data packets are managed in communication networks. At each DER, randomization is injected to the packet request process based on its local dynamic state, which limits synchronization between DERs and promotes equitable access to the grid. In addition, the DER is endowed with opt-out logic to guarantee quality of service (QoS) for the end-consumer (e.g., no worse than conventional device control). Figure 1 illustrates the standard closed-loop system under PEM.

The following high-level description summarizes the bottom-up approach that is PEM and is detailed in [19], [20]:

1. A DER measures its local dynamic state (e.g., energy).
2. If the state exceeds a locally defined limit, the DER exits PEM, reverts to a default DER control mode until the state is returned to within limits and returns to Step 1. Else, based on the state, the DER probabilistically requests to consume (inject) energy at a fixed rate from (into) the grid for a pre-specified epoch (i.e, an *energy packet*).
3. The aggregator (or *Virtual Power Plant*, VPP) either accepts or denies the DER's packet request based on grid or market conditions, such as power reference tracking error or grid capacity constraints. If request is denied, return to Step 1. If accepted, the DER consumes (injects) energy for the epoch and returns to Step 1.

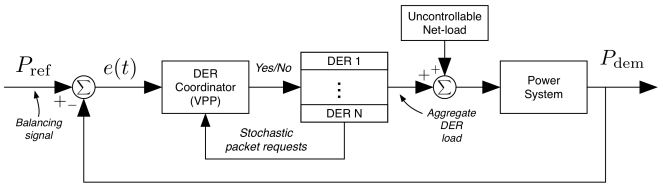


Figure 1. Closed-loop feedback system for PEM with $P_{\text{ref}}(t)$ provided by the grid or market operator and the aggregate net-load $P_{\text{dem}}(t)$ measured by VPP.

In a fleet of diverse DERs (e.g., TCLs and batteries), one considers that the general discrete-time dynamic model for the $n$-th DER having energy state $z_n$ is given by

$$z_n^+ = f_n(z_n, \phi_n, P_{\text{c},n}^{\text{rate}}, P_{\text{d},n}^{\text{rate}}, w_n), \tag{1}$$

where $f_n$ is some one-dimensional nonlinear mapping (usually linear or bilinear), $w_n$ is the parameter mapping end-consumer usage to the energy state, $P_{\text{c},n}^{\text{rate}}$ and $P_{\text{d},n}^{\text{rate}}$ are the energy transfer rates of the $n$-th DER when charging (c) or discharging (d), respectively, and $\phi_n$ is the hybrid state corresponding to the set of modes {charge, standby, discharge} [19], [20]. In this paper, the focus is put on TCLs (electric water heaters or EWHs) and ESSs. For example, when the $n$-th ESS has $w_n = 1$ and $P_{\text{c},n}^{\text{rate}}, P_{\text{d},n}^{\text{rate}} > 0$, (1) becomes

$$z_n^+ = \eta_{\text{sl},n} z_n + \eta_{\text{c},n} P_{\text{c},n}^{\text{rate}} - \eta_{\text{d},n} P_{\text{d},n}^{\text{rate}}, \tag{2}$$

where $\eta_{\text{sl},n}$, $\eta_{\text{c},n}$, and $\eta_{\text{d},n}$ are the standing losses, charging, and discharging parameters, respectively.

The probability that the $n$-th packetized DER with local dynamic state at time $k$, satisfying $z_n[k] \in [\underline{z}_n, \overline{z}_n]$ and desired set-point $z_n^{\text{set}} \in (\underline{z}_n, \overline{z}_n)$ requests access to the grid during interval $\Delta t$ is defined by the cumulative exponential distribution function $P(z_n[k]) := 1 - e^{-\mu(z_n[k])\Delta t}$, where the rate parameter $\mu(z_n[k]) > 0$ is dependent on the local dynamic state. Denoting by $P_k^{\text{h}}(n|\Gamma)$ the probability that load $n$ requests a packet for consumption (h = c) or injection (h = d) given condition $\Gamma$ is satisfied. The following boundary conditions establishes the dependence between local dynamic state and the request probability:

$$i)\ \ P_k^{\text{c}}\left(n|\, z_n[k] \le \underline{z}_n\right) = 1 \qquad P_k^{\text{c}}\left(n|\, z_n[k] \ge \overline{z}_n\right) = 0,$$

$$ii)\ \ P_k^{\text{d}}\left(n|\, z_n[k] \le \underline{z}_n\right) = 0 \qquad P_k^{\text{d}}\left(n|\, z_n[k] \ge \overline{z}_n\right) = 1.$$

For an ESS consuming (c) packets for ESS, $i)$ gives

$$\mu(z_n[k]) = \begin{cases} 0, & \text{if } z_n[k] \ge \overline{z}_n \\ m_R \left(\frac{\overline{z}_n - z_n[k]}{z_n[k] - \underline{z}_n}\right) \cdot \left(\frac{z_n^{\text{set}} - \underline{z}_n}{\overline{z}_n - z_n^{\text{set}}}\right), & \text{if } z_n[k] \in (\underline{z}_n, \overline{z}_n) \\ \infty, & \text{if } z_n[k] \le \underline{z}_n \end{cases} \tag{3}$$

where $m_R > 0$ [Hz] is a design parameter that defines the mean time-to-request (MTTR). For example, if one desires a MTTR of 5 minutes when $z_n[k] \equiv z_n^{\text{set}}$ then $m_R = \frac{1}{600}$Hz. The design of $\mu(z_n[k])$ for *injecting* a packet is described in similar fashion, but with boundary conditions $ii)$ above. Figure 2 maps boundary conditions to charging and discharging packet requests.

In [20], a bin transition model was developed for a population of diverse DERs under PEM. The model is provided below for the sake of completeness. Let $\bar{\mathcal{X}} = \{x_1, \ldots, x_N\}$ constitute a consecutively ordered partitioning of $[\underline{z}, \overline{z}]$. Assume

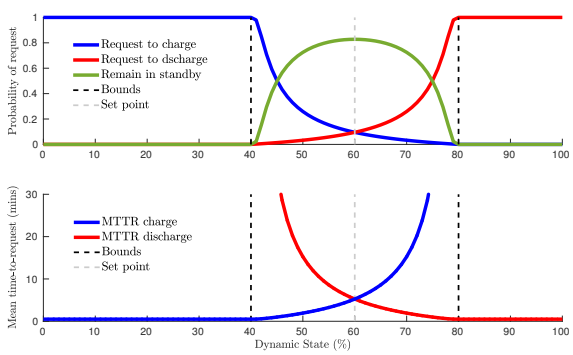


Figure 2. Illustrating the charge/discharge energy packet request rates and MTTR for a generic packetized load. Note that (3) is represented by the blue line (left to right top plot). Top plot gives the effect of local state $z_n$ (e.g., state-of-charge) on the packet request probabilities and bottom plot provides the corresponding MTTR of a packetized DER under PEM.

that there exists an appropriate probability space $(\Omega, P, \mathcal{F})$, where $\Omega$ is the set of events, $\mathcal{F}$ a filtration, and $P$ the probability measure of elements in $\mathcal{F}$. Then, random variables $\{X_k\}_{k\geq 0}$ are defined as $X_k : \Omega \to \mathcal{X}$. Let $x_j \in \mathcal{X}$ and denote $q_j[k] = P(X_k = x_j)$ as the probability of $X_k = x_j$, $k \geq 0$. The column vector $q[k] := (q_1, \ldots, q_N)^T$ then gives the probability mass function of the random variable $X_k$. Also, the transition probabilities between states are denoted as $p_{ij} = P(X_{k+1} = x_i | X_k = x_j)$. Since (1) includes three types of dynamics (i.e., charge/standby/discharge), the state space for the system consists of the union of three identical copies of $\bar{\mathcal{X}}$. That is, the full state space is given by $\mathcal{X} = \mathcal{X}_{\mathrm{c}} \cup \mathcal{X}_{\mathrm{sb}} \cup \mathcal{X}_{\mathrm{d}}$. At time $k$, the probability mass function of the system is $q^\top = (q_{\mathrm{c}}^\top, q_{\mathrm{sb}}^\top, q_{\mathrm{d}}^\top)$ with $q_{\mathrm{c}} = (q_{\mathrm{c}}^1, \cdots, q_{\mathrm{c}}^N)^\top$ and $q_{\mathrm{sb}}$ and $q_{\mathrm{d}}$ defined similarly. Note that $q$ contains the percentage of the population in each state of $\mathcal{X}$.

The bilinear system equations are then

$$q[k+1] = M \underbrace{\left(I + M^+_{\beta[k]} + M^-_{\beta^-[k]}\right)}_{=: \tilde{M}\left(\beta[k], \beta^-[k]\right)} q[k], \tag{4a}$$

$$y[k] = c^\top q[k], \tag{4b}$$

where the two-dimensional control signal $\beta := (\beta_{\mathrm{c}}, \beta_{\mathrm{d}})$ defines the proportion of DERs moving from standby to charge (c) and discharge (d), and $\beta^- := (\beta_{\mathrm{c}}^-, \beta_{\mathrm{d}}^-)$ is the proportion of DERs whose charge (c) and discharge (d) packets end and return to standby. The matrix $M := \mathrm{diag}\{M_{\text{exit-}\oplus}, \bar{M}, M_{\text{exit-}\ominus}\}$, where $M_{\text{exit-}\oplus}$ correspond to the natural transition of the opt-out population and $M_{\text{exit-}\ominus}$ introduces the transition probabilities to re-enter PEM in standby mode,

$$\bar{M} = \left(\begin{array}{c|c|c} M_{\mathrm{c}} & M_{\mathrm{c,sb}} & 0_N \\ \hline M_{\mathrm{sb,c}} & M_{\mathrm{sb}} & M_{\mathrm{d,sb}} \\ \hline 0_N & 0_N & M_{\mathrm{d}} \end{array}\right), \quad M^-_\beta := \left(\begin{array}{c|c|c} \beta_{\mathrm{c}}^- I_N & 0_N & 0_N \\ \hline -\beta_{\mathrm{c}}^- I_N & 0_N & -\beta_{\mathrm{d}}^- I_N \\ \hline 0_N & 0_N & \beta_{\mathrm{d}}^- I_N \end{array}\right),$$

$$M^+_\beta := \left(\begin{array}{c|c|c} 0_N & \beta_{\mathrm{c}} T_{\text{req,c,}\backslash\mathrm{d}} & 0_N \\ \hline 0_N & -\beta_{\mathrm{c}} T_{\text{req,c,}\backslash\mathrm{d}} - \beta_{\mathrm{d}} T_{\text{req,d,}\backslash\mathrm{c}} & 0_N \\ \hline 0_N & \beta_{\mathrm{d}} T_{\text{req,d,}\backslash\mathrm{c}} & 0_N \end{array}\right),$$

the diagonal blocks in $\bar{M}$ (i.e., $M_{\mathrm{h}}$, for $\mathrm{h} = \{\mathrm{c}, \mathrm{sb}, \mathrm{d}\}$) are tridiagonal matrices describing the state bin transition probabilities, the off-diagonal blocks are given by $M_{\mathrm{c,sb}} = e_1 e_1^\top p_{\mathrm{c}}^{\mathrm{sb}}$, $M_{\mathrm{sb,c}} = e_N e_N^\top p_{\mathrm{sb}}^{\mathrm{c}}$, $M_{\mathrm{d,sb}} = e_N e_N^\top p_{\mathrm{d}}^{\mathrm{sb}}$, $e_i$ denotes the $i$-th standard basis vector, $0_N$ and $I_N$ are the standard $N \times N$ zero and identity matrices, $T_{\text{req,c,}\backslash\mathrm{d}}$ is a diagonal matrix containing the probabilities of charging packet requests given that no discharging request has been made using (3), and $T_{\text{req,}\backslash\mathrm{c,d}}$ is a diagonal matrix containing the probabilities of discharging packet requests given that no charging request has been made. In particular, $M_{\text{exit-}\ominus}$ and $M_{\text{exit-}\oplus}$ ensure that the dynamic state of DERs remain within the specified limits.

Modeling the evolution of the number of active DER charging and discharging packets in the system introduces two sets of timer states (c and d). That is, given packet epoch $\delta$, the sampling time step $\Delta t$, and two timer states vectors $x_{p,\mathrm{h}} \in \mathbb{R}^{n_p}$ with $n_p = \lfloor \delta / \Delta t \rfloor$ and $\mathrm{h} = \{\mathrm{c}, \mathrm{d}\}$, the *timer dynamics* are given by

$$x_{p,\mathrm{h}}[k+1] = M_{p,\mathrm{h}} x_{p,\mathrm{h}}[k] + C_{p,\mathrm{h}}\, q_{\mathrm{h}}^+[k], \tag{5}$$

where $q_{\mathrm{h}}^+ := \beta_{\mathrm{h}} T_{\mathrm{req,h}} q_{\mathrm{sb}} = \beta_{\mathrm{h}} \bar{q}_{\mathrm{sb}}^{\mathrm{h}}$, $T_{\mathrm{req},c} = T_{\text{req,c,}\backslash\mathrm{d}}$, $T_{\mathrm{req},d} = T_{\text{req,}\backslash\mathrm{c,d}}$ and $C_{p,\mathrm{h}} \in \mathbb{R}^{n_p \times N}$ is responsible for allocating the new charge/discharge population into their corresponding charge/discharge timer states. The number of charging/discharging packet requests received by the VPP is then $n_r^{\mathrm{h}} := \mathbf{1}_N^\top \bar{q}_{\mathrm{sb}}^{\mathrm{h}}$ with $\mathrm{h} = \{\mathrm{c}, \mathrm{d}\}$ and $\mathbf{1}_N = (1, \ldots, 1)^\top \in \mathbb{R}^N$. The timer provides the formula for the percentage of DERs whose packet expires. That is, $\beta_{\mathrm{h}}^- := x_{p,\mathrm{h}}^{(n_p)} / \sum_{i=1}^{n_p} x_{p,\mathrm{h}}^{(i)}$, where $x_{p,\mathrm{h}}^{(i)}$ is the $i$-th component of $x_{p,\mathrm{h}}$. A depiction of a DER population under PEM is provided in Fig. 3.

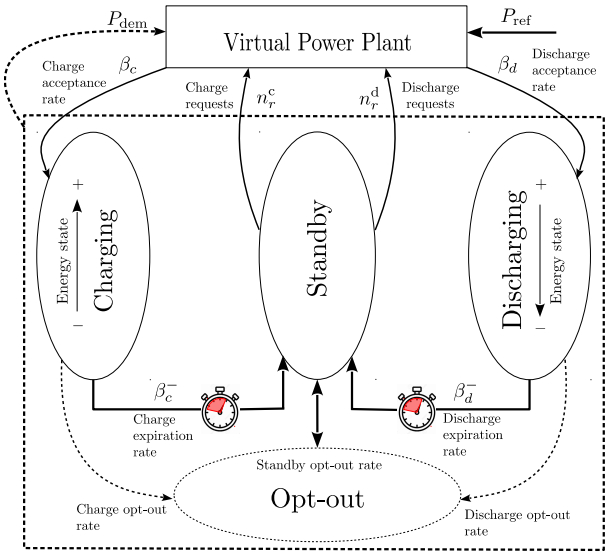


Figure 3. Transition diagram of a DER population under PEM.

## III. Reference Tracking and Packet Requests

This section provides an explicit control law for real-time reference tracking by the aggregated PEM system described in Section II. The control law determines the proportion of charging and discharging requests that are accepted (i.e., $\beta = (\beta_c, \beta_d)$) and is straightforward: 1) measure the tracking error (reference signal minus net-demand) and 2) accept enough requests so that this error is minimized. This logic is similar

to a relay-based control system, except the "relay" in the PEM macroscopic model is continuous in $[0,1]$, which reflects the underlying binary response logic from the VPP to the device's request: {deny, accept}. That is, the VPP indirectly transitions proportions of the DER population between different modes while keeping DERs completely anonymous and avoid prioritizing requests from certain bins over the rest. Recall that for each time step $k$, each request can include its corresponding charge/discharge energy transfer limit, e.g., $P^{\text{rate}}_{\text{h},n}$, which provides the VPP with the estimate $P^{\text{rate}}_{\text{h}} := \frac{1}{\beta_{\text{h}} n^{\text{h}}_r} \sum_{n=1}^{\beta_{\text{h}} n^{\text{h}}_r} P^{\text{rate}}_{\text{h},n}$ for $\text{h} = \{\text{c,d}\}$. Let $P_{\text{ref}}$ be the reference power signal provided by some grid or market operator and let $P_{\text{dem}}$ be the measured VPP net-load. The two scalar control inputs $\beta_{\text{c}}$ and $\beta_{\text{d}}$ are generated by the VPP to minimize the tracking error and at the same time maximize the number of accepted charging requests $\chi_{\text{c}}$ and discharging requests $\chi_{\text{d}}$. That is, the VPP solves the following quadratic programming problem for time step $k$:

$$\chi^*_{\text{c}}, \chi^*_{\text{d}} = \underset{\substack{\chi_{\text{c}} \in [0, n^{\text{c}}_r[k]] \\ \chi_{\text{d}} \in [0, n^{\text{d}}_r[k]]}}{\operatorname{argmin}} \; (\mathcal{F}(\chi)[k])^2 \tag{6}$$

where $\mathcal{F}(\chi)[k] = \chi_{\text{c}} P^{\text{rate}}_{\text{c}}[k] - \chi_{\text{d}} P^{\text{rate}}_{\text{d}}[k] - \epsilon[k]$ and $\epsilon[k] := P_{\text{ref}}[k] - P_{\text{dem}}[k]$ is the tracking error of the VPP. Thus, $\beta_{\text{c}}[k] = \chi^*_{\text{c}}/n^{\text{c}}_r[k]$ and $\beta_{\text{d}}[k] = \chi^*_{\text{d}}/n^{\text{d}}_r[k]$. The solution to (6) is provided in the theorem below [1].

*Theorem 1:* Define

$$n_{\text{error}}[k] = \begin{cases} \dfrac{\epsilon[k]}{P^{\text{rate}}_{\text{c}}}, & \epsilon[k] \geq 0 \\ \dfrac{|\epsilon[k]|}{P^{\text{rate}}_{\text{d}}}, & \epsilon[k] < 0. \end{cases}$$

The solution to (6) that maximizes the number of accepted requests for $\epsilon[k] > 0$ is given by

$$\chi_{\text{c}} = \begin{cases} \min\left\{ n^{\text{c}}_r, \frac{(n^{\text{d}}_r P^{\text{rate}}_{\text{d}} + \epsilon)}{P^{\text{rate}}_{\text{c}}} \right\}, & n^{\text{c}}_r > n_{\text{error}}, \\ n^{\text{c}}_r, & n^{\text{c}}_r \leq n_{\text{error}}, \end{cases}$$

$$\chi_{\text{d}} = \begin{cases} \min\left\{ \frac{(n^{\text{c}}_r P^{\text{rate}}_{\text{c}} - \epsilon)}{P^{\text{rate}}_{\text{d}}}, n^{\text{d}}_r \right\}, & n^{\text{c}}_r > n_{\text{error}}, \\ 0, & n^{\text{c}}_r \leq n_{\text{error}}, \end{cases}$$

The case when $\epsilon[k] < 0$ is similar for $n_{\text{d}}$. The proof of Theorem 1 is omitted here due to space constraints but it follows directly from convexity and KKT conditions.

Figure 4 presents the application of Theorem 1 to a tracking VPP with 2000 packetized devices that maximizes the total number of accepted packets each time instant $k$.

## IV. Packet completion and steady state

In this section, selected system properties of PEM are detailed for the first time. The first property focuses in the mechanics of expiring packets, which is related to the VPP timers that keep track of the number of DERs transitioning from c/d mode to standby mode. The second property relates to direct computation of the nominal PEM control that exactly positions the mean dynamic state of DERs at the desired set-point.

[1]Note that $\mathcal{F}(\chi)$ is only positive semi-definite. Thus, the optimal solution may not be unique.

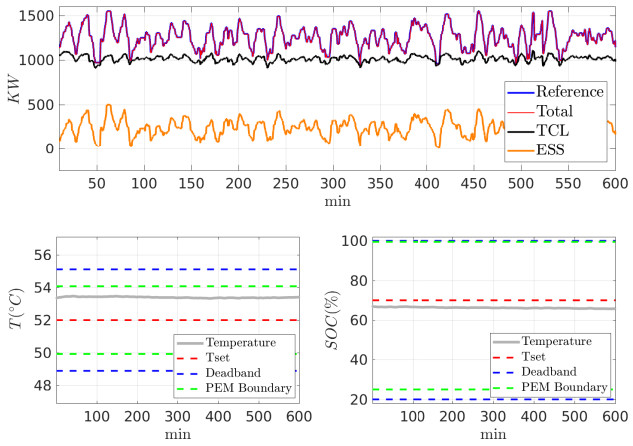


Figure 4. Applying Theorem 1 to a VPP that employs a fleet of 1000 TCLs and 1000 ESSs whose parameters are provided in [20], [21]. The VPP is tracking a detrended and scaled automatic generator control (AGC) dispatch signal from ISO New England [22]

### A. Packet completion rates

The existence of a stationary distribution for (4) when $\beta_{\text{c}}$ and $\beta_{\text{d}}$ are constant inputs is straightforward since the PEM system was designed to be described by an irreducible and aperiodic Markov chain model. A control law for $\beta_{\text{c}}$ and $\beta_{\text{d}}$ was provided in the previous section, therefore, the interest of this section is on the steady state behavior of the signals $\beta^-_{\text{c}}$ and $\beta^-_{\text{d}}$. The analysis focuses on $\beta^-_{\text{c}}$ as case $\beta^-_{\text{d}}$ is similar. Below it is shown that, at steady-state, $\beta^-_{\text{c}}$ is a constant scalar that depends on the number of timer bins and how packet interruptions are designed by matrix $C_{\text{p,h}}$ in (5).

Assume that control $\beta_{\text{c}}$ is fixed and (4) has reached its stationary distribution. Recall from (5) that $q^+_{\text{c}} = \beta_{\text{c}} T_{\text{req,c,d}} q_{\text{sb}} = \beta_{\text{c}} \bar{q}^{\text{c}}_{\text{sb}}$, and note that the $j$-th component of $x_{p,\text{c}}$ is

$$x^{(j)}_{p,\text{c}}[k] = x^{(j-1)}_{p,\text{c}}[k-1] + \beta_{\text{c}} C^{(j)}_{p,\text{c}} \bar{q}^{\text{c}}_{\text{sb}}[k-1],$$

where $C^{(j)}_{p,\text{c}}$ is the $j$-th row of $C_{p,\text{c}}$. Iterating $j-1$ times gives

$$x^{(j)}_{p,\text{c}}[k] = \underbrace{x^{(1)}_{p}[k-j-1]}_{\beta_{\text{c}} C^{(1)}_{p,\text{c}} \bar{q}^{\text{c}}_{\text{sb}}[k-j-2]} + \beta_{\text{c}} \sum_{i=0}^{j-2} C^{(j-i)}_{p,\text{c}} \bar{q}^{\text{c}}_{\text{sb}}[k-i-1]$$

By definition,

$$\beta^-_{\text{c}}[k] = \frac{x^{(n_p)}_{p,\text{c}}[k]}{\sum_{j=1}^{n_p} x^{(j)}_{p,\text{c}}[k]} = \frac{\beta_{\text{c}} \sum_{i=0}^{n_p-1} C^{(n_p-i)}_{p,\text{c}} \bar{q}^{\text{c}}_{\text{sb}}[k-i-1]}{\sum_{j=1}^{n_p} \beta_{\text{c}} \sum_{i=0}^{j-1} C^{(j-i)}_{p,\text{c}} \bar{q}^{\text{c}}_{\text{sb}}[k-i-1]}.$$

Under the assumption of stationarity, it follows that

$$\beta^-_{\text{c}} = \frac{\left( \sum_{i=0}^{n_p-1} C^{(n_p-i)}_{p,\text{c}} \right) \bar{q}^{\text{c}}_{\text{sb}}}{\left( \sum_{j=1}^{n_p} \sum_{i=0}^{j-1} C^{(j-i)}_{p,\text{c}} \right) \bar{q}^{\text{c}}_{\text{sb}}} = \frac{C_1 \bar{q}^{\text{c}}_{\text{sb}}}{C_2 \bar{q}^{\text{c}}_{\text{sb}}}.$$

It is only left to show that $\beta^-_{\text{c}}$ is independent of $q$. Observe that $C_1, C_2 \in \mathbb{R}^{1 \times N}$ and $\bar{q}^{\text{c}}_{\text{sb}} \in \mathbb{R}^N$ have all positive components. Also, $C_i \bar{q}^{\text{c}}_{\text{sb}} = \text{Tr}(C_i \bar{q}^{\text{c}}_{\text{sb}}) = \text{Tr}(\bar{q}^{\text{c}}_{\text{sb}} C_i)$ and $C_i C^{\dagger}_i = 1$, where $\text{Tr}(\cdot)$ and $(\cdot)^{\dagger}$ denote the trace operator and the Moore-Penrose

pseudo inverse, respectively. In particular $C_i^\dagger = C_i^\top/(C_i C_i^T)$. It then follows that

$$\begin{aligned}\beta_{\rm c}^-[k] &= \frac{C_1\bar{q}_{\rm sb}^{\rm c}}{C_2\bar{q}_{\rm sb}^{\rm c}} = \frac{\mathrm{Tr}(C_1\bar{q}_{\rm sb}^{\rm c}C_2C_2^\dagger)}{\mathrm{Tr}(C_2\bar{q}_{\rm sb}^{\rm c})} = \frac{\mathrm{Tr}(C_2^\dagger C_1\bar{q}_{\rm sb}^{\rm c}C_2)}{\mathrm{Tr}(C_2\bar{q}_{\rm sb}^{\rm c})} \\ &\le \lambda_{\max}(C_2^\dagger C_1)\frac{\mathrm{Tr}(\bar{q}_{\rm sb}^{\rm c}C_2)}{\mathrm{Tr}(C_2\bar{q}_{\rm sb}^{\rm c})} = \lambda_{\max}(C_2^\dagger C_1) \\ &\le C_1C_2^\dagger.\end{aligned}$$

The inequality above follows since all matrices involved are positive semidefinite and rank one. In the simple case without packet interruptions, one has $C_p^{(i)} = (0,\cdots,0)$ for $i = 2,\ldots,n_p$ implying $C_1 = C_p^{(1)}$ and $C_2 = n_pC_p^{(1)}$. This gives $\beta_{\rm c}^- = 1/n_p$ in the stationary distribution.

*Example 1:* Consider a system in steady state with $\beta_{\rm c} = \beta_{\rm d} = 1$ (to increase packet interruption rate) and a timer with $n_p = 20$ bins. The analytic upper bound for a fixed $C_{p,{\rm c}} \in \mathbb{R}^{n_p\times N}$ is 0.0515 whereas a direct simulation show $\beta_{\rm c}^- = 0.0507$. Without packet interruptions, $\beta_{\rm c}^- = 0.05 = \frac{1}{n_p}$. □

**Remark:** Simulations suggest that within the capacity of the system (low opt-out rates) the values of $\beta_{\rm c}^-$ and $\beta_{\rm d}^-$ remain close to $1/n_p$. Figure 5 shows such observation when tracking a sinusoidal reference using Theorem 1. This suggests future work on a simplified model is derived ignoring the rational dynamics of $\beta_{\rm c}^-$ and $\beta_{\rm d}^-$ by approximating both as $1/n_p$.

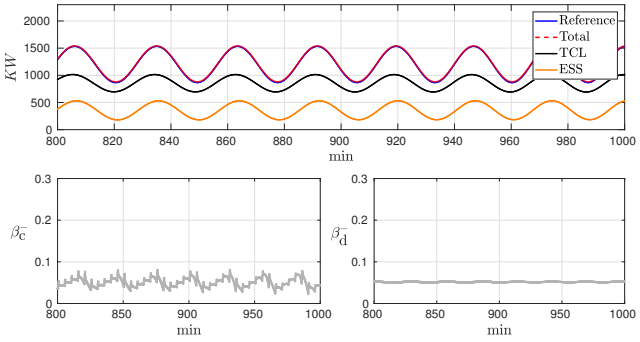


Figure 5. Depicting the long term behavior of $\beta_{\rm c}^-$ and $\beta_{\rm d}^-$ when tracking a sinusoid with PEM. Notice that $\beta_{\rm c}^-, \beta_{\rm d}^- \approx \frac{1}{n_p} = 0.05$.

### B. Nominal response of PEM system

When manipulating resources, such as DERs, the grid operator must consider the minimal power output level of the VPP that provides flexibility for tracking and at the same time allows for each individual DER to satisfy its needs. In this vein, a definition for the *nominal response* of a PEM system is given.

*Definition 1:* The nominal response of a VPP under PEM described as in (4) is the minimum constant power signal for which QoS is sufficiently satisfied for the average DER under PEM.

Knowing this nominal response provides a baseline over which flexibility can be measured [23], [24], and establishes the first step in the development of a virtual energy storage model that is capable of providing ancillary services to grid operators through DERs. This nominal behavior is characterized in terms of the *nominal control* $\beta^* = (\beta_{\rm c}^*, \beta_{\rm d}^*)$ that is the

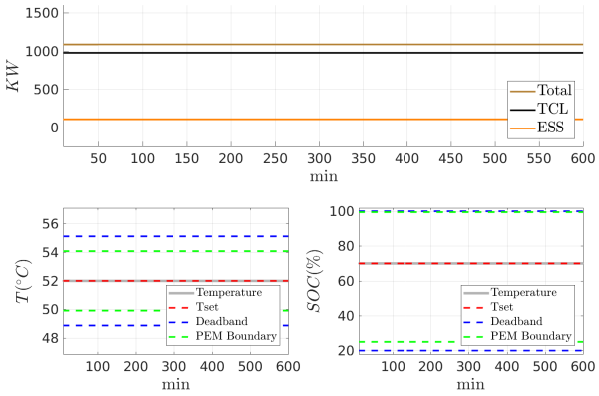


Figure 6. QoS positioning of DERs for a VPP with 1000 TCLs and 1000 ESSs. The mean dynamic state of each DER population satisfies (7c) with equality for the specified population set points with nominal control $\beta_{\rm c}^* = 0.206$ and $\beta_{\rm d}^* = 0.145$.

solution of the following nonlinear non-convex optimization problem:

$$\beta_{\rm c}^*, \beta_{\rm d}^* = \underset{\beta_{\rm c},\beta_{\rm d}\in[0,1]}{\operatorname{argmin}} \sum_{i=1}^{n} P_i \quad \text{subject to} \tag{7a}$$

$$q_i^* = M\tilde{M}(\beta,\beta^-)\,q_i^*, \tag{7b}$$

$$(q_i^*)^\top x_{\rm v}^i \ge z_{\rm set}^i, \tag{7c}$$

where $P_i = C_iq_i^*$ is the demand power corresponding to the $i$-th class of DERs when at steady state provided by $q_i^*$, $x_{\rm v}^i \in \mathcal{X}^i$ is the vector of values (e.g., temperature, SOC, etc) associated to the bins of the $i$-th DER class, $z_{\rm set}^i$ is the desired set point for the dynamic state of the $i$th DER class. As showed in Section IV-A and since packet interruptions are negligible when the mean dynamic state sits at the set-point, it is reasonable to assume $\beta_{\rm c}^- = 1/n_p = \beta_{\rm d}^-$. For $\beta_{\rm c}$ and $\beta_{\rm d}$ constant, a stationary distribution is guaranteed to exist from (7), which implies that (7b) always possess a solution. An observation that allows for this problem to be solved is that $\sum_{i=1}^n P_i$ is a monotone function with respect to $\beta_{\rm c}, \beta_{\rm d}$. Similarly, the average dynamic state $(q_i^*)^\top x_{\rm v}^i$ varies monotonically as a function of $\beta_{\rm c}, \beta_{\rm d}$ for any DER class $i$. Additionally, recall that the solution space is limited to $\beta_{\rm c}, \beta_{\rm d} \in [0,1]$. Therefore, there exist a unique solution for (7). Figure 6 depicts this nominal response of a VPP with two DER populations (TCLs and ESS). In the case of more than two DER populations, the nominal response may not always correspond to QoS at the specified set point. However, the average dynamic states will always be above those desired set points, which satisfies QoS.

**Remark:** Interestingly, the nominal control $\beta_{\rm c}^*$ and $\beta_{\rm d}^*$ is invariant with respect to the proportion of the DER classes and the number of devices in each DER population. It only depends on the parameters of (4), including packet length and height and sampling time, and, thus, provides a viable avenue for constructing a virtual energy storage model of a VPP.

## V. Observability and EKF for PEM

A critical aspect in demand dispatch techniques such as the ones in [4], [5] is to infer the bin distribution out of limited information shared by DERs. PEM is no different in this aspect, which amounts to the property of observability for

the PEM system (4). Thus, this section focuses on studying the observability of the PEM system, where only power and number of charging/discharging requests is shared. The state equation (4a) can be rewritten as a discrete-time bilinear system:

$$q[k+1] = Aq[k] + \sum_{i=1}^{m} u_i[k] N_i q[k] =: A_{u[k]} q[k], \quad (8a)$$

$$y[k] = CP(k, u[k])\, q[0], \quad (8b)$$

where $q[k]$ is the distribution of DERs in each bin of the system at time-step $k$, $u[k] \in \mathcal{U} \subseteq [0,1]^m$ is the control input over time step $k$, and matrices $A, N_i$ and $C$ can be easily obtained from the description in Section II. Note that $P(k, u[k]) := A_{u[k]} \cdots A_{u[1]}$ and $P(0, u[k]) := I$, $\forall k \in \mathbb{N}$ recursively describes the $k$-step state prediction. It is usually the case that $u = \{\beta_{\mathrm{c}}, \beta_{\mathrm{c}}^{-}, \beta_{\mathrm{d}}, \beta_{\mathrm{d}}^{-}\}$, which makes $m = 4$ (for the case of only EWHs $u = \{\beta_{\mathrm{c}}, \beta_{\mathrm{c}}^{-}\}$, i.e., $m = 2$). Note that system (8) have $\beta_{\mathrm{c}}^{-}$ and $\beta_{\mathrm{d}}^{-}$ as "free" inputs as is the case for the systems in [4], [5], where these inputs serve for switching DERs from ON to OFF. Due to the full knowledge of the timer states by the PEM VPP, the focus is in the free case for $\beta_{\mathrm{c}}^{-}$ and $\beta_{\mathrm{d}}^{-}$. Observability of (8) is now described in terms of observability of linear time varying systems [25].

*Definition 2:* System (8) is called observable on the time interval $[0, T]$ if any initial state $x[0] = x_0$ is uniquely determined by the corresponding response $y[k]$ for $k = 0, \ldots, T$.

Define the observability Gramian matrix as

$$\mathcal{W}_{k,u} := \sum_{j=0}^{k} Z_{j,u[k]} = \sum_{j=0}^{k} P(j, u[k])^{\top} C^{\top} C P(j, u[k]) \quad (9)$$

Note that $\mathcal{W}_{k,u} q[0] = \sum_{j=0}^{k} P(j, u[k])^{\top} C^{\top} y[k]$. Also, $Z_{k,u}$ satisfies $Z_{k+1,u} = A_{u[k]}^{\top} Z_{k,u} A_{u[k]}$ with $Z_{0,u} = C^{\top} C$. If the observability Gramian is nonsingular, then

$$q[0] = (\mathcal{W}_{k,u})^{-1} \sum_{j=0}^{k} P(j, u[k])^{\top} C^{\top} y[k].$$

Defining $\mathcal{O}_{0,T} = (C^{\top} \;\; P^{\top}(1, u[k]) C^{\top} \;\; \cdots \;\; P^{\top}(T, u[k]) C^{\top})^{\top}$, one has that $\mathcal{W}_{T,u} = \mathcal{O}_{0,T}^{\top} \mathcal{O}_{0,T}$. In this context, observability is rephrased in the next definition.

*Definition 3:* System (8) is observable if there exist an input sequence on the interval $[0, T]$ such that $\mathcal{W}_{k,u}$ is positive definite.

The property of observability can be attained or is kept if $[0, T]$ is incremented. On the contrary, it can be lost by reducing the time interval. It was also shown in [26] that a randomized piecewise constant input sequence act as universal inputs for bilinear systems. From [27], one can also test for observability geometrically, by checking that $\operatorname{rank}(\bar{\mathcal{O}}_n) = n$ where $\bar{\mathcal{O}}_1 = C$, $\bar{\mathcal{O}}_i = \left(A^{\top} \bar{\mathcal{O}}_{i-1}^{\top} \;\; N_1^{\top} \bar{\mathcal{O}}_{i-1}^{\top} \;\; \cdots \;\; N_m^{\top} \bar{\mathcal{O}}_{i-1}^{\top}\right)^{\top}$. The PEM system has been designed in a manner that Definition 2 holds even in the case that $\beta_{\mathrm{c}} = \beta_{\mathrm{d}} = 0$. For instance, all $A_u$ and $P(k, u)$ matrices are stochastic and correspond to irreducible and aperiodic (due to self-loops) discrete Markov chains. The next example illustrates the observability property for a PEM system.

*Example 2:* Consider a fleet of TCLs whose deadband is partitioned into 4 dynamic state bins (see [21, (10) and (12)] for more details on TCLs). Since TCLs do not produce discharging requests the natural evolution of DERs is provided by the transition matrix

$$M = \begin{pmatrix} 0.1 & 0 & 0 & 0 & 0.3 & 0 & 0 & 0 \\ 0.9 & 0.1 & 0 & 0 & 0 & 0 & 0 & 0 \\ 0 & 0.9 & 0.1 & 0 & 0 & 0 & 0 & 0 \\ 0 & 0 & 0.9 & 0.2 & 0 & 0 & 0 & 0 \\ 0 & 0 & 0 & 0 & 0.7 & 0.1 & 0 & 0 \\ 0 & 0 & 0 & 0 & 0 & 0.9 & 0.1 & 0 \\ 0 & 0 & 0 & 0 & 0 & 0 & 0.9 & 0.1 \\ 0 & 0 & 0 & 0.8 & 0 & 0 & 0 & 0.9. \end{pmatrix},$$

where the entries of $M$ are indicative of TCLs. The expression for the instantaneous switching of DERs governed by the VPP is

$$\bar{M}(\beta, \beta^{-}) = I_{2N} + \beta_{\mathrm{c}} \underbrace{\begin{pmatrix} 0_N & T_{\mathrm{req}} \\ 0_N & T_{\mathrm{req}} \end{pmatrix}}_{=: \bar{N}_1} + \beta_{\mathrm{c}}^{-} \underbrace{\begin{pmatrix} -I_N & 0_N \\ I_N & 0_N \end{pmatrix}}_{=: \bar{N}_2},$$

where $C = (1, 1, 1, 1, 0, 0, 0, 0)$, and the probability of requests matrix is $T_{\mathrm{req}} = \operatorname{diag}\{0.99, 0.6, 0.2, 0.05\}$. Here $A = M$, $N_1 = M\bar{N}_1$, $N_2 = M\bar{N}_2$, $m = 2$, $u_1 = \beta_{\mathrm{c}}$, and $u_2 = \beta_{\mathrm{c}}^{-}$. One can easily show that for any randomly chosen $u_1 \in [0, 1]$ and $u_2 \in [0, 1/n_p]$ ($n_p = 20$ timer bins), the maximum input sequence length needed for achieving observability is 7. An experiment was performed in which the system was run for 2000 random input sequences. Sequences of at least length 2 to at most length 7 are needed for the system to become observable. Even in the case when $\beta_{\mathrm{c}}^{-}$ is fixed as per Section IV-A the maximum input sequence needed has length 7. For simplicity, the system in this example did not considered opt-out dynamics [20], [21]. However, even with opt-out included, if observability is lost, then one can increase the observation interval $[0, T]$ until observability is recovered. Finally, the rank test for observability, in this example, is also satisfied for $n = 8$. This example holds for any non-zero choice of the components of $M$ as long as the matrix structures given in (4) are preserved. □

With the bilinear PEM system being observable, convergence of an observer algorithm is guaranteed. To take into account measurement noise, one can formulate an Extended Kalman Filter (EKF) observer for system (8). The extended Kalman filter is usually given in two stages:

*i*. Measurement update:

$$K[k] = \mathrm{Cov}[k|k-1] C^{\top} (C \mathrm{Cov}[k|k-1] C^{\top} + R_1[k])^{-1}$$
$$\hat{q}[k|k] = \hat{q}[k|k-1] + K[k](y[k] - C\hat{q}[k|k-1])$$
$$\mathrm{Cov}[k|k] = \mathrm{Cov}[k|k-1] - K[k] C \mathrm{Cov}[k|k-1]$$

*ii*. Time update:

$$\hat{q}[k+1|k] = A_{u[k]} \hat{q}[k|k]$$
$$\mathrm{Cov}[k+1|k] = A_{u[k]} \mathrm{Cov}[k|k] A_{u[k]}^{\top} + R_2[k],$$

where $\hat{q}[k|k-1]$ is the predicted state of the system state, $\hat{q}[k|k]$ is the most recent estimate of the system state, $\mathrm{Cov}[k|k-1]$ denotes the predicted system covariance, $\mathrm{Cov}[k|k]$ denotes the current system covariance estimation, $R_1$ is the measurement noise covariance and $R_2$ is the time update noise covariance. The convergence parameters for time-varying linear system are trivial [28, Section III]. Figure 7 illustrates how the EKF is able to accurately estimate the output power and also the number of charging/discharging packet requests.

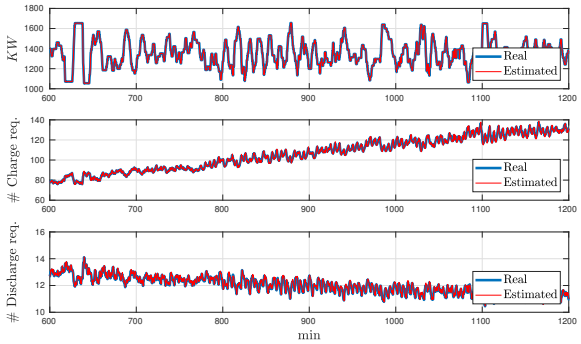


Figure 7. EKF estimation of aggregate power output and charging and discharging packet requests for a VPP coordinating 1000 TCLs and 1000 ESSs while tracking ISO-NE AGC reference signal [22].

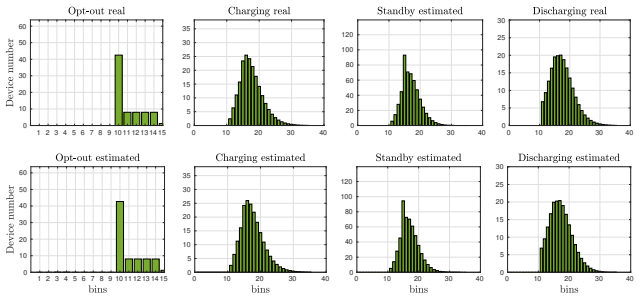


Figure 8. Illustrating the high accuracy of EKF estimation for ESS population at minute 1000, which is representative of overall performance for ESSs and TCLs.

Also, in Fig. 8 a snapshot of ESS distributions is shown for minute 1000 of the simulation for the opt-out, charging, standby and discharging populations.

## VI. Conclusions

This paper presents the systematic analysis for a model of the aggregate system response of a population of diverse distributed energy resources based on a bottom-up energy request methodology known as packetized energy management (PEM). Future work will build on these results to derive PEM performance guarantees by quantifying the VPP family of reference signals that can be tracked and position available VPP flexibility for techno-economic power system objectives.

## References


[1] M. Morgan and S. Talukdar, "Electric power load management: Some technical, economic, regulatory and social issues," *Proceedings of the IEEE*, vol. 67, no. 2, pp. 241–312, Feb. 1979.

[2] F. C. Schweppe, R. D. Tabors, J. L. Kirtley, H. R. Outhred, F. H. Pickel, and A. J. Cox, "Homeostatic utility control," *Transactions on Power Apparatus and Systems*, no. 3, pp. 1151–1163, May 1980.

[3] D. S. Callaway and I. A. Hiskens, "Achieving Controllability of Electric Loads," *Proceedings of the IEEE*, vol. 99, no. 1, pp. 184–199, Jan. 2011.

[4] J. L. Mathieu, S. Koch, and D. S. Callaway, "State Estimation and Control of Electric Loads to Manage Real-Time Energy Imbalance," *Transactions on Power Systems*, vol. 28, no. 1, pp. 430–440, Nov. 2013.

[5] S. P. Meyn, P. Barooah, A. Busic, Y. Chen, and J. Ehren, "Ancillary Service to the Grid Using Intelligent Deferrable Loads," *Transactions on Automatic Control*, vol. 60, no. 11, pp. 2847–2862, Nov. 2015.

[6] M. Vrakopoulou, J. L. Mathieu, and G. Andersson, "Stochastic Optimal Power Flow with Uncertain Reserves from Demand Response," in *47th Hawaii International Conference on System Sciences*, Mar. 2014, pp. 2353–2362.

[7] G. S. Ledva and J. Mathieu, "A Linear Approach to Manage Input Delays While Supplying Frequency Regulation Using Residential Loads," in *2017 American Control Conference*, May 2017, pp. 1–7.

[8] J. L. Mathieu, M. Kamgarpour, J. Lygeros, and D. S. Callaway, "Energy arbitrage with thermostatically controlled loads," in *European Conference on Circuit Theory and Design*, July 2013, pp. 2519–2526.

[9] W. Zhang, J. Lian, C. Y. Chang, K. Kalsi, and Y. Sun, "Reduced order modeling of aggregated thermostatic loads with demand response," in *51st Conference on Decision and Control*, Dec. 2012, pp. 5592–5597.

[10] W. Zhang, J. Lian, C.-Y. Chang, and K. Kalsi, "Aggregated Modeling and Control of Air Conditioning Loads for Demand Response," *Transactions on Power Systems*, vol. 28, no. 4, pp. 4655–4664, Oct. 2013.

[11] S. Esmaeil Zadeh Soudjani and A. Abate, "Aggregation and Control of Populations of Thermostatically Controlled Loads by Formal Abstractions," *Transactions on Control Systems Technology*, vol. 23, no. 3, pp. 975–990, May 2015.

[12] S. P. Meyn, P. Barooah, A. Busic, and J. Ehren, "Ancillary service to the grid from deferrable loads: The case for intelligent pool pumps in Florida," in *52nd Conference on Decision and Control*, Dec. 2013, pp. 6946–6953.

[13] A. Busic, M. U. Hashmi, and S. P. Meyn, "Distributed control of a fleet of batteries," in *2017 American Control Conference*, May 2017, pp. 3406–3411.

[14] Y. Chen, A. Busic, and S. P. Meyn, "State estimation and mean field control with application to demand dispatch," in *54th Conference on Decision and Control*, Dec. 2015, pp. 6548–6555.

[15] N. Mahdavi, J. Braslavsky, and C. Perfumo, "Mapping the Effect of Ambient Temperature on the Power Demand of Populations of Air Conditioners," *Transactions on Smart Grid*, vol. 99, pp. 1–11, Jul. 2016.

[16] B. Zhang and J. Baillieul, "Control and Communication Protocols Based on Packetized Direct Load Control in Smart Building Microgrids," *Proceedings of the IEEE*, vol. 104, no. 4, pp. 837–857, Apr. 2016.

[17] M. K. Petersen, L. H. Hansen, J. Bendtsen, K. Edlund, and J. Stoustrup, "Heuristic Optimization for the Discrete Virtual Power Plant Dispatch Problem," *Transactions on Smart Grid*, vol. 5, no. 6, pp. 2910–2918, Nov. 2014.

[18] J. A. Chekan and S. Bashash, "IOT-Oriented Control of Aggregate Thermostatically-Controlled Loads*," in *2017 American Control Conference*, May 2017, pp. 1–6.

[19] M. Almassalkhi, J. Frolik, and P. Hines, "Packetized energy management: Asynchronous and anonymous coordination of thermostatically controlled loads," in *2017 American Control Conference*, May 2017, pp. 1431–1437.

[20] L. A. Duffaut Espinosa, M. Almassalkhi, P. Hines, and J. Frolik, "Aggregate modeling and coordination of diverse energy resources under packetized energy management," in *56th Conference on Decision and Control*, Dec. 2017, pp. 1394–1400.

[21] L. A. Duffaut Espinosa, M. Almassalkhi, P. Hines, S. Heydari, and J. Frolik, "Towards a macromodel for packetized energy management of resistive water heaters," *51st Conference on Information Sciences and Systems*, Mar. 2017.

[22] ISO New England, "Simulated Automatic Generator Control (AGC) Setpoint Data: Energy Neutral," https://www.iso-ne.com/isoexpress/web/reports/grid/-/tree/simulated-agc, Last Accessed: 2017-10-18.

[23] H. Hao, B. M. Sanandaji, K. Poolla, and T. L. Vincent, "Aggregate flexibility of thermostatically controlled loads," *Transactions on Power Systems*, vol. 30, no. 1, pp. 189–198, Jan. 2015.

[24] J. L. Mathieu, M. Kamgarpour, J. Lygeros, and D. S. Callaway, "Energy arbitrage with thermostatically controlled loads," in *2013 European Control Conference*, July 2013, pp. 2519–2526.

[25] W. J. Rugh, *Linear system theory*, 2nd ed. Upper Saddle River, N.J.: Prentice Hall, 1996.

[26] P. Sen, "On the choice of input for observability in bilinear systems," *Transactions on Automatic Control*, vol. 26, no. 2, pp. 451–454, Apr. 1981.

[27] A. Isidori, "Direct construction of minimal bilinear realizations from nonlinear input-output maps," *Transactions on Automatic Control*, vol. 18, no. 6, pp. 626–631, Dec. 1973.

[28] M. Boutayeb, H. Rafaralahy, and M. Darouach, "Convergence analysis of the extended kalman filter used as an observer for nonlinear deterministic discrete-time systems," *Transactions on Automatic Control*, vol. 42, no. 4, pp. 581–586, Apr. 1997.